Supporting Information

Highly Efficient and Stable $CsPbBr_3$ Perovskite Quantum Dots by Encapsulating in Dual-Shell Hollow Silica Spheres for WLEDs

Lei Qiu, [a] Hang Yang, [a] Zhigao Dai, [a] Fengxu Sun, [a] Jiarui Hao, [a] Mengyu Guan, [a] Peipei Dang, [b] Chunjie Yan,*[a] Jun Lin*[b, c] and Guogang Li*[a]

a. Engineering Research Center of Nano-Geomaterials of Ministry of Education, Faculty of Materials Science and Chemistry, China University of Geosciences, 388 Lumo Road, Wuhan 430074, P. R. China.

b. State Key Laboratory of Rare Earth Resource Utilization, Changchun Institute of Applied Chemistry, Chinese Academy of Sciences, Changchun 130022, P. R. China.

c. School of Applied Physics and Materials, Wuyi University, Jiangmen, Guangdong, 529020, P. R. China

E-mail: ggli@cug.edu.cn; chjyan@cug.edu.cn; jlin@ciac.ac.cn

Figures and Tables Content

Results and discussion

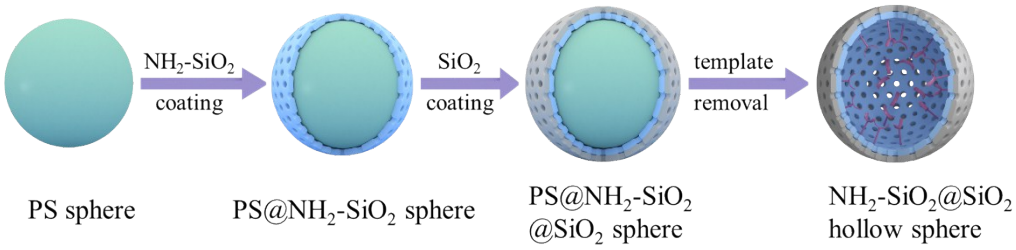

Figure S1. The stepwise fabrication process of dual-shell hollow SiO_2 spheres via a simple successive ionic layer adsorption and reaction (SILAR) method.

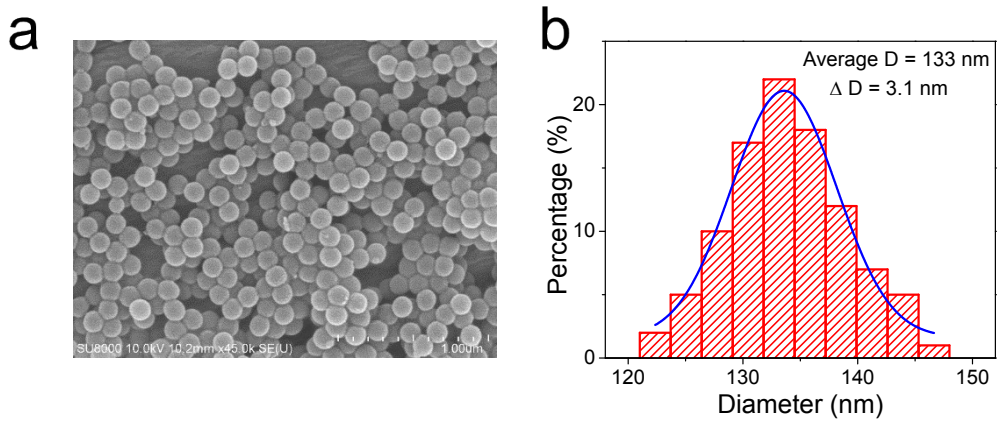

Figure S2. (a) The SEM images of presynthesized PS spheres. (b) The size distribution of PS spheres with an average size of 133 nm.

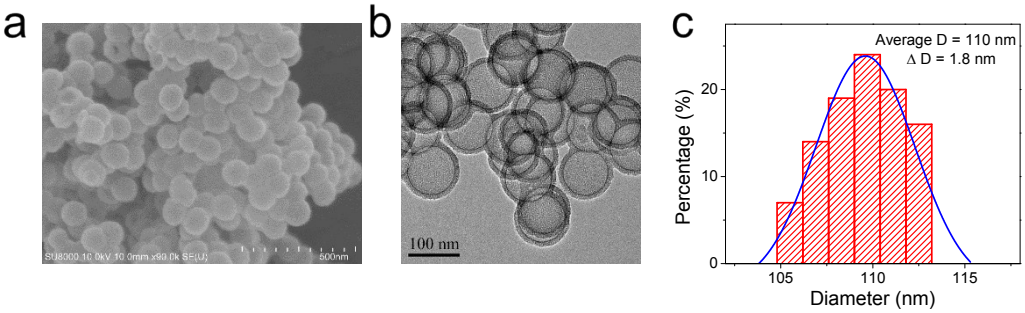

Figure S3. (a) The SEM and (b) TEM images of as-prepared SiO_2-2 spheres. (b) The size distribution of SiO_2-2 spheres with an average size of 110 nm.

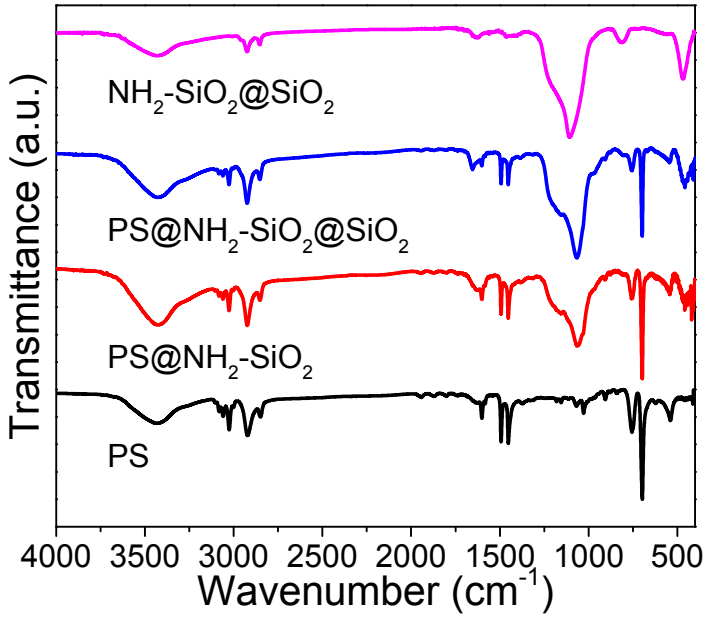

Figure S4. The FTIR spectra of PS, PS@NH_2-SiO_2, PS@NH_2-SiO_2@SiO_2 and NH_2-SiO_2@SiO_2.

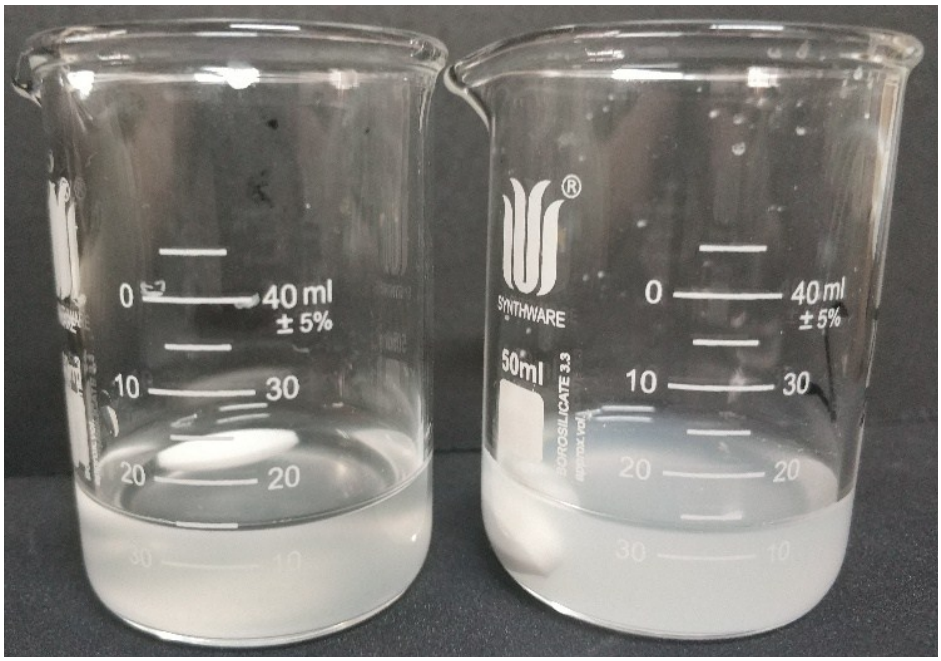

Figure S5. The photographs of SiO_2-0 (left) and SiO_2-2 (right) aqueous solution with adsorption of Pb^{2+} for 20 min.

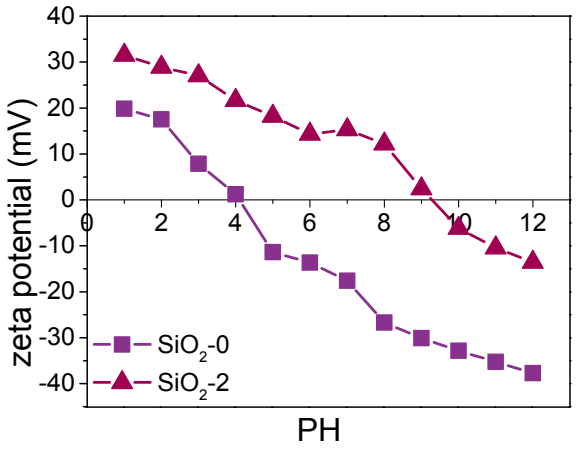

Figure S6. The zeta potential analysis of SiO_2-0 and SiO_2-2.

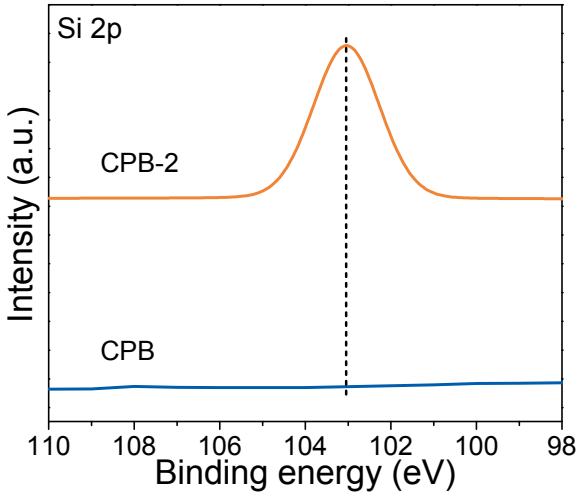

Figure S7. High-resolution XPS spectra of Si 2p.

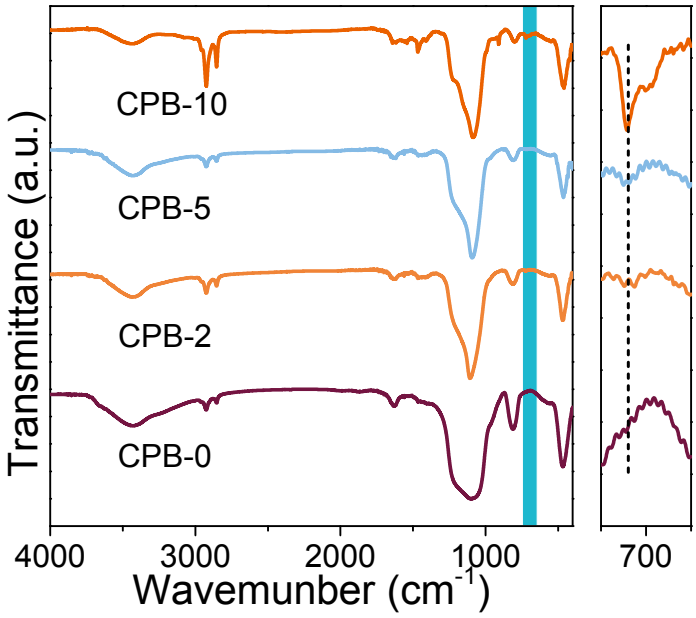

Figure S8. The FTIR spectra of CPB-0, CPB-2, CPB-5 and CPB-10.

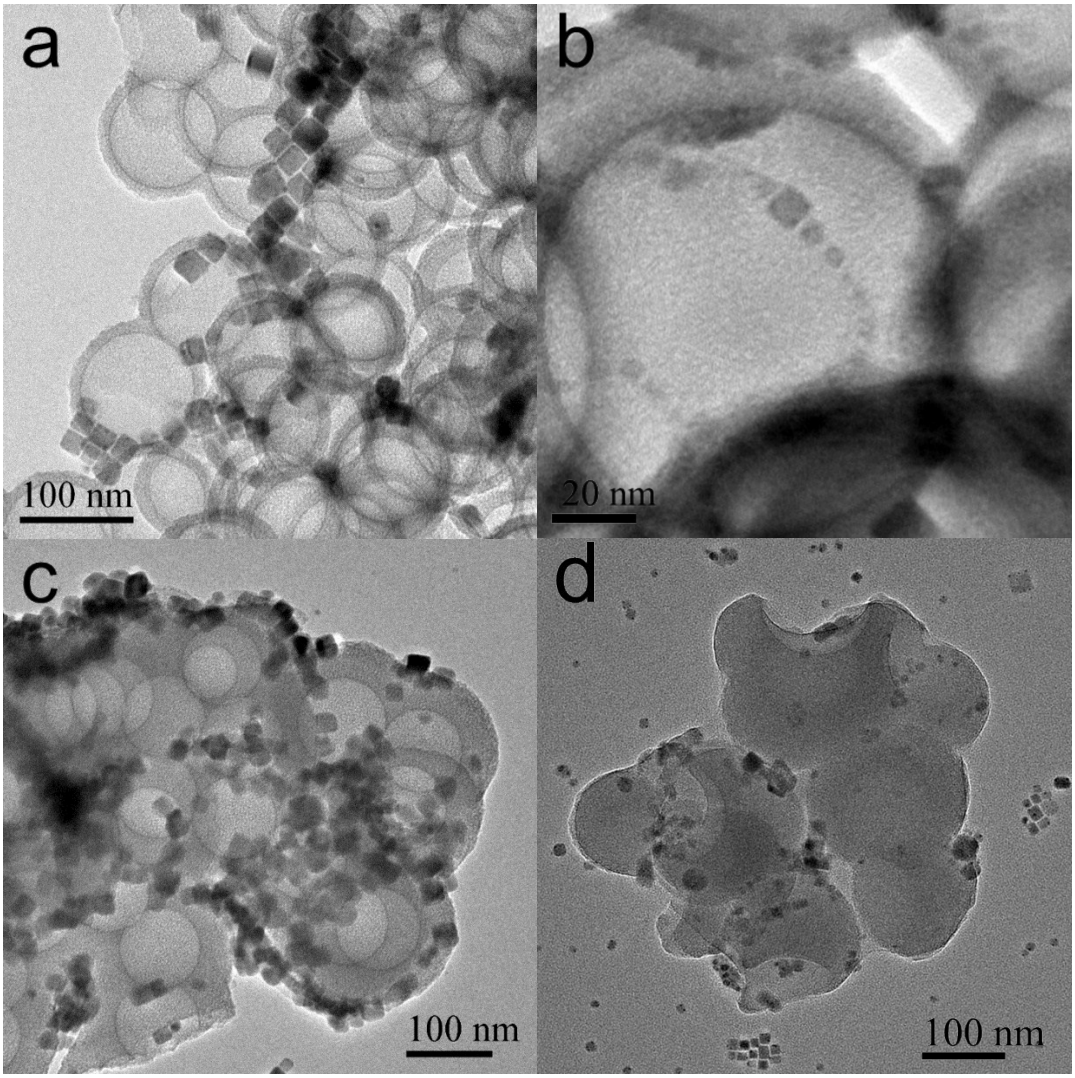

Figure S9. TEM images of (a) CPB-0, (b) CPB-2, (c) CPB-5 and (d) CPB-10.

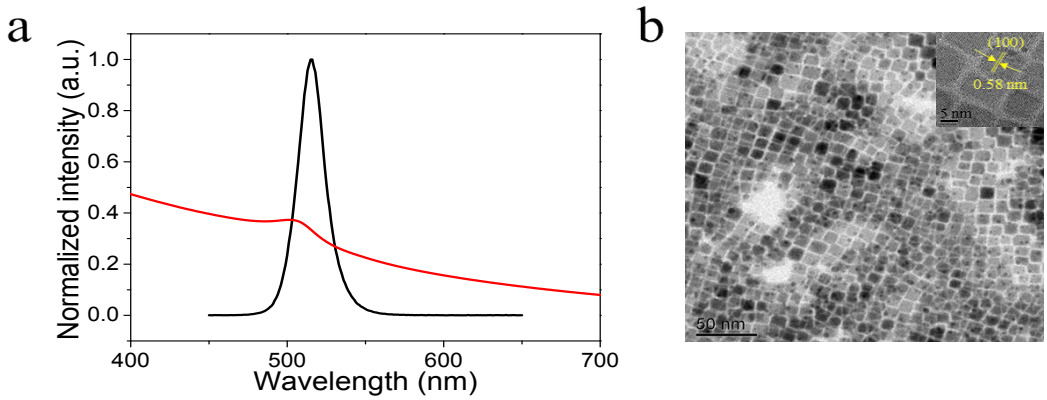

Figure S10. The (a) PL spectra (black line), absorption spectra (red line) and (b) TEM image of pure $CsPbBr_3$ QDs.

It could be observed that the emission peak of pure $CsPbBr_3$ QDs is 516 nm and the absorption edges lock at 510 nm. The emission peak of pure $CsPbBr_3$ QDs keeps the same with amino-free CPB-0, but is slight red shift for CPB-2, CPB-5 and CPB-10, which demonstrate the passivation effect of amino-groups may hinder the growth of $CsPbBr_3$ QDs. The TEM images of pure $CsPbBr_3$ QDs shown in Figure S10b indicate a lattice distance of 0.58 nm, which corresponding to (100) plane of cubic $CsPbBr_3$ QDs.

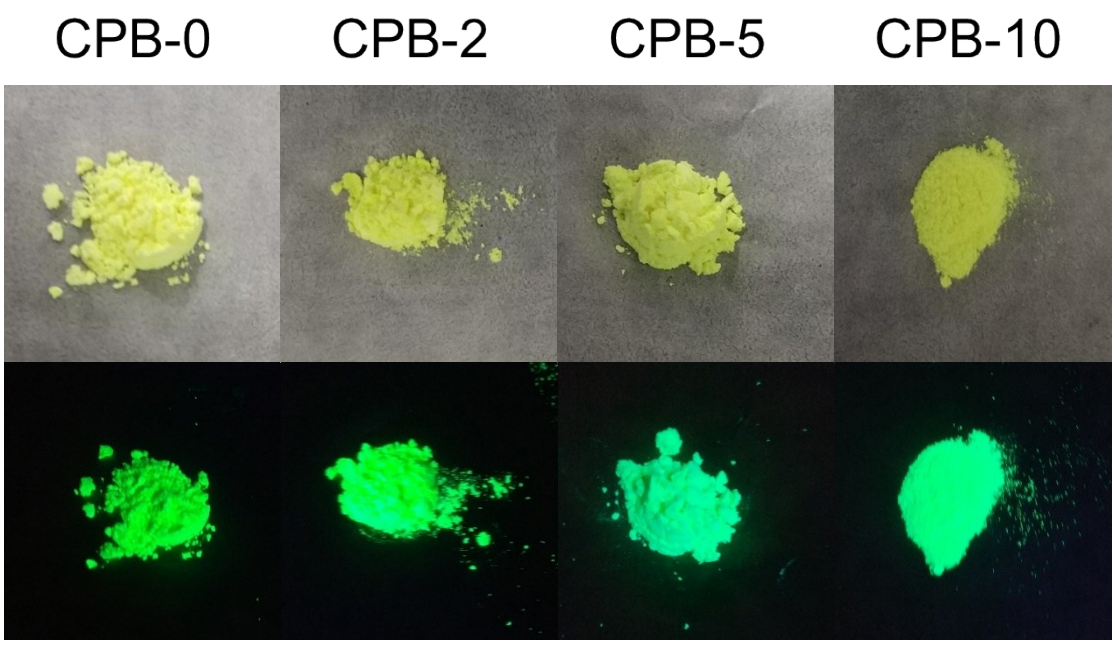

Figure S11. The photographs of CPB-0, CPB-2, CPB-5 and CPB-10 under daylight (top) and UV light (bottom).

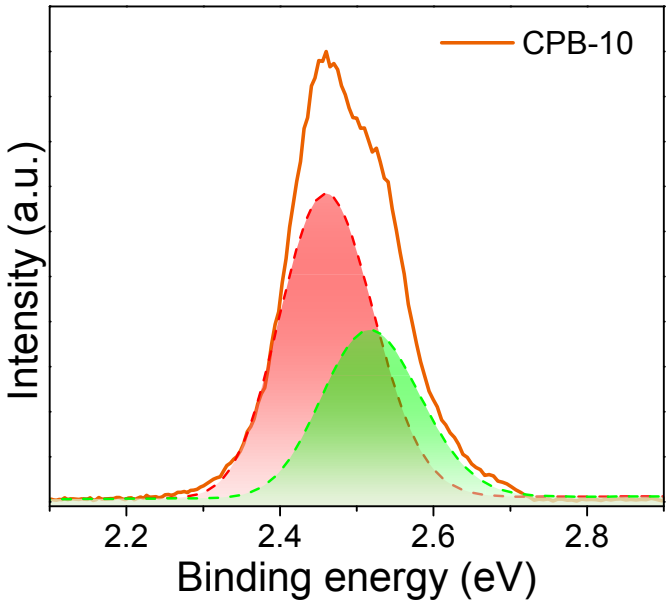

Figure S12. The Guassian fitting peaks of CPB-10.

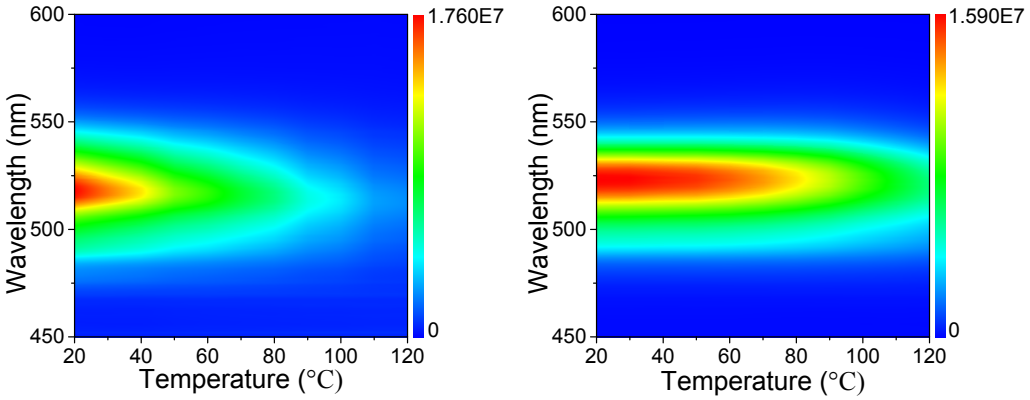

Figure S13. Temperature dependent PL intensity of pure CPB (left) and CPB-2 (right) at different wavelengths.

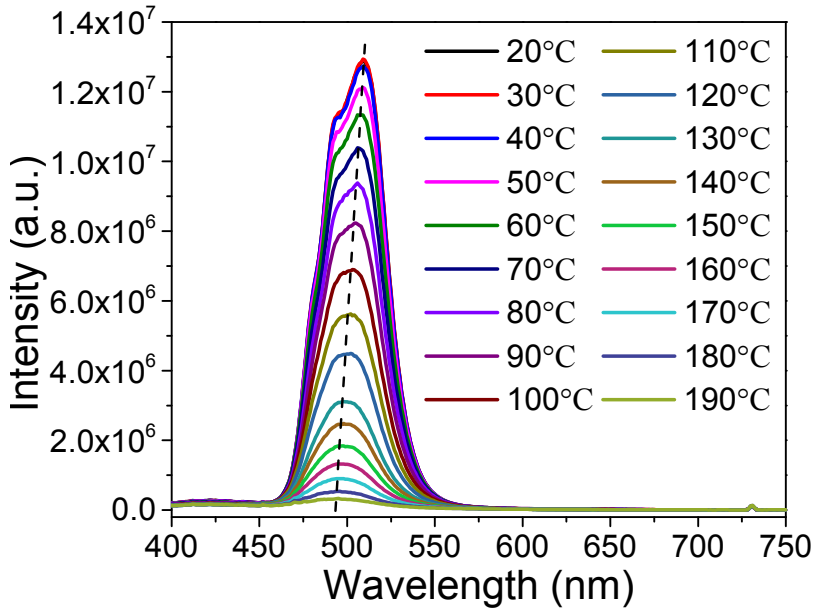

Figure S14. Temperature dependent PL spectra of CPB-2 ranging from 20 to 190°**C**.

Table S1. The measured values of Pb^{2+} concentrations and calculated adsorption percentage of SiO_2-0 and SiO_2-2 with various time intervals.

Time/min	SiO_2-0		SiO_2-2	
	measured value/(μg/mL)	adsorption percentage/%	measured value/(μg/mL)	adsorption percentage/%
0	25	0	25	0
5	24.0374	3.8504	21.4582	14.1672
10	23.3292	6.6832	18.6433	25.4268
20	22.6526	9.3896	15.8864	36.4544
30	22.2281	11.0876	15.4642	38.1432
40	22.0236	11.9056	15.5222	37.9112
50	21.9869	12.0524	15.4397	38.2412
60	22.0018	11.9254	15.4551	38.1796

Table S2. The optical characters of CPB-0, CPB-2, CPB-5 and CPB-10.

Samples	Absorption peak/nm	PL peak/nm	FWHM/nm	PLQY/%	Abs	τ_{avg}/ns
CPB-0	(456, 513)	516	35	58.5	0.596	7.53
CPB-2	(449, 485)	512	41	88.9	0.602	11.61
CPB-5	(408, 472)	504	29	32.0	0.652	9.35
CPB-10	(424, 472)	504	32	31.3	0.398	5.58